International Journal of Affective Engineering Vol.XX No.X pp.XXX-XXX (20XX)
doi: 10.5057/ijae.IJAE-D-XX-XXXXX

Type of the Paper

A Differential Equation Model of Anxiety and Habituation Based on Allergic Responses and Its Computational Simulation Using Real-World Social Data

Kota OHNO [1*], Kunio SHIMIZU [2], Satoshi FUKUDA [1], and Hiroko SHOJI [1†]

[1] Chuo University, 1-3-27 Kasuga, Bunkyo-ku, Tokyo 112-8551, Japan
[2] The Institute of Statistical Mathematics, 10-3 Midori-cho, Tachikawa, Tokyo 190-8562, Japan

[*]Corresponding author, E-mail: kohno737@g.chuo-u.ac.jp
[†] JSKE Member

Received: XXXX.XX.XX
Accepted: XXXX.XX.XX
J-STAGE Advance Publish Date: XXXX.XX.XX

Copyright: © 20XX by the authors. Submitted for possible open access publication under the terms and conditions of the Creative Commons Attribution (CC BY) license (https://creativecommons.org/licenses/by/4.0/).

Preprint: (if necessary): An early preprint is available on XXXX (https://xxxx/xxxx.xxxxx).

This article is part of the Special Issue on XXXX 20XX. (if necessary)

Abstract: We propose a mathematical model for the dynamics of anxiety that incorporates implicit habituation based on an analogy with allergic responses. Quantifying emotions such as anxiety remains challenging because objective information does not necessarily reflect people's subjective anxiety. Anxiety also decreases when people are repeatedly exposed to similar information, a phenomenon analogous to immunotherapy for allergic responses. Our model incorporates the interaction between anxiety and implicit habituation based on this mechanism. We applied the model to anxiety related to the COVID-19 pandemic and successfully reproduced the reduced increase in anxiety under repeated exposure to similar stimuli. The proposed mathematical model provides a new perspective for understanding KANSEI dynamics.
Keywords: KANSEI modeling, COVID-19, SNS data, Differential equation, numerical simulation

1. Introduction

People often experience subjective anxiety triggered by objective information. Examples include social information expressed numerical values, such as the number of newly infected people during the COVID-19 pandemic. Objective information can trigger subjective anxiety; however, the resulting emotion does not necessarily correspond to the information itself. This study analyzes changes in subjective anxiety in response to objective information. We propose a mathematical model, described by differential equations, to represent the relationship between subjective anxiety and objective information. Furthermore, our model demonstrates the dynamics of anxiety and predicted future trends.

People's anxiety is often not triggered by objective information when they are repeatedly exposed to the same information. This phenomenon, in which responses weaken with repeated stimulation, is called "habituation." Several studies have investigated this phenomenon. Regarding neural responses to physical stimulation, Horn reported an experimental study on the habituation of a single neuron (Horn, 1967). Psychological studies have also examined emotional responses and habituation. For instance, Ariga proposed an experimental model showing that people become distracted and their attention decreases when performing parallel tasks (Ariga & Lleras, 2011).

Stanley introduced a classical mathematical approach to habituation and proposed a neural model in which responses decay exponentially (Stanley, 1976). In emotion research, a statistical model describing emotional dynamics and habituation phenomena has also been proposed based on the free-energy principle (Ueda et al., 2021). From the perspective of repeated exposure to information, Bartkow et al. analyzed information propagation using a mathematical model of epidemic disease transmission (Bartkow et al., 2023).

As previously mentioned, habituation related to emotions has been widely reported. However, in this study, we propose a mathematical model based on the allergic-response framework from a novel perspective: the dynamic interaction between anxiety and habituation is analogous to the allergic response (Ohno & Shoji, 2023). Allergic symptoms, such as sneezing and difficulty in breathing, are caused by exposure to allergens such as pollen and food. Exposure to allergens increases Th2 cells, which induce allergic symptoms, and Treg cells, which suppress the increase in Th2 cells. The generation of Th2 cells induces allergic symptoms; however, appropriately generated Treg cells suppress the increase in Th2 cells and prevent allergic symptoms onset. This mechanism forms the basis of immunotherapy for allergic responses. Through long-term exposure to controlled amounts of allergens, Treg cells gradually increase, preventing allergic symptoms even during exposure to high allergen levels, such as during pollen season. This type of immunotherapy has been investigated using mathematical models (Fishman & Segel, 1996; Groß et al., 2011). In particular, Hara proposed a simple two-component model representing the interaction between Th2 cells and Treg cells (Hara & Iwasa, 2017).

Throughout this study, habituation is conceptualized as tolerance to anxiety. The emotional system underlying anxiety and habituation resembles the allergic-response system. Specifically, the increase in Th2 cells induced by allergen exposure is analogous to the increase in anxiety triggered by objective information, whereas the effect of Treg cells is analogous to habituation to anxiety. When prior anxiety-related information is available, the increase in subjective anxiety is suppressed. Consequently, exposure to highly anxiety-inducing objective information may not elicit subjective anxiety because habituation has developed through long-term exposure to similar information. Based on this concept, we proposed a mathematical model that describes this system using an immunotherapy framework (Ohno & Shoji, 2023). The model demonstrated the dynamics of anxiety and habituation through numerical simulations using hypothetical information, and the numerical results were interpreted using COVID-19-related anxiety as an example.

In this study, we used the number of newly confirmed COVID-19 cases as objective information and related posts on social network services (SNS) as response to this information. The SNS data revealed an initial increase in subjective anxiety that gradually declined with long-term exposure to objective information. Furthermore, we proposed a modified mathematical model that reflects the characteristics of this phenomenon. Numerical simulations confirmed that our mathematical model, using COVID-19 data as input information, qualitatively reproduced the dynamics of subjective anxiety. Based on a statistical evaluation of the numerical results, our differential equation-based model suggested that people's subjective anxiety gradually shifts toward habituation.

2. Data and Preliminary Analysis

In this study, we used the number of newly confirmed COVID-19 cases (Ministry of Health, Labor and Welfare, n.d.) as objective information, along with reply posts from SNS. The COVID-19 data represent information that induces anxiety, whereas the SNS data represent people's responses to this information.

2.1 Number of newly confirmed COVID-19 cases

The COVID-19 data were obtained from publicly available open data. The investigation period spanned from January 1, 2020, to May 8, 2023. These data were aggregated daily. In this study, we used the number of newly confirmed COVID-19 cases in Tokyo. This choice was related to the reply post data, as are explained later.

2.2 Definition of the epidemic period

We defined the epidemic period based on the increases and decreases in the COVID-19 data. Here, x_i denotes the raw COVID-19 data, and the epidemic period is defined according to the following rules:

1. Calculate the one-week moving average:
$$p_i = \frac{1}{7}\sum_{j=i-3}^{i+3} x_j.$$
2. Convert to logarithmic scale:
$$y_i = \log(1 + p_i).$$
3. Select candidates for peaks and valleys:
   A candidate peak satisfies $y_t > y_{t-1}\ and\ y_t > y_{t+1}$,
   while a candidate valley satisfies $y_t < y_{t-1}\ and\ y_t < y_{t+1}$.
4. Extract peaks and valleys from the candidates that satisfy the following conditions:
$$y_i^{\text{high}} - \min\left(y_{i-1}^{\text{low}}, y_i^{\text{low}}\right) \geq \rho$$
$$\max\left(y_{i-1}^{\text{high}}, y_i^{\text{high}}\right) - y_i^{\text{low}} \geq \rho$$
   Here, ρ denotes the threshold of prominence, and i denotes the index of a peak or valley.
5. Definition of an epidemic period:

A sequence of valley → peak → valley was defined as a single epidemic period. Therefore, when expressed in days, a single epidemic period is given by $[t_i^{\mathrm{low}}, t_{i+1}^{\mathrm{low}}]$ (Table 1).

In Figure 1, the background colors are assigned based on this definition and the orange points indicate the peak timing, and the green points indicate valley timing.

Table 1. Start and end dates of each epidemic period.

	Start date (t_i^{low})	End date (t_{i+1}^{low})
1st	2020/5/20	2020/9/22
2nd	2020/9/22	2021/3/5
3rd	2021/3/5	2021/6/12
4th	2021/6/12	2021/11/25
5th	2021/11/25	2022/5/3

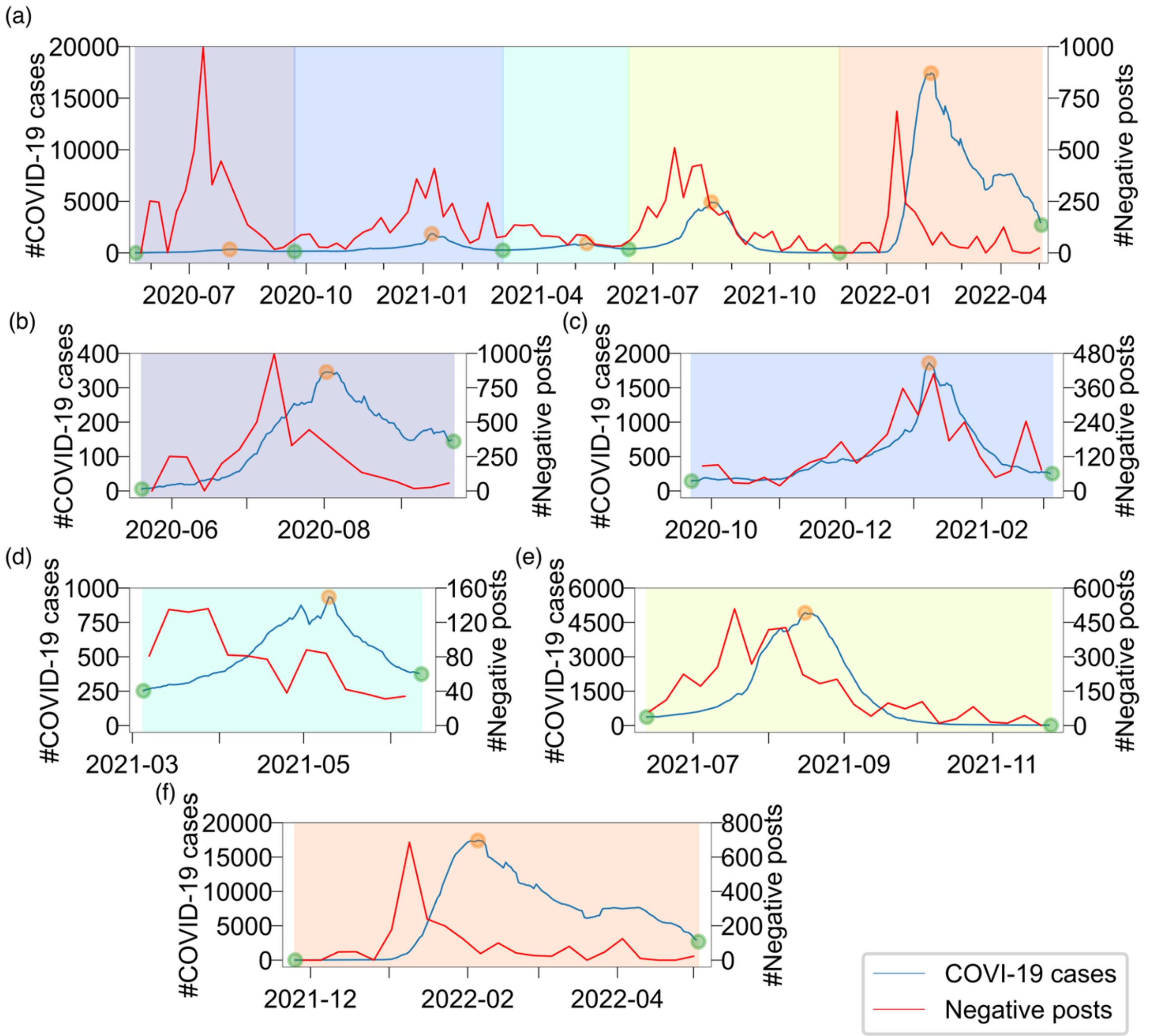

Figure 1 Time profiles of the number of newly confirmed COVID-19 cases and negative reply posts. Panel (a) corresponds to the entire period. Panels (b)–(f) correspond to the first through fifth periods, respectively. The blue line represents the number of newly confirmed COVID-19 cases, whereas the red line represents the number of negative reply posts. The background colors indicate the epidemic periods. Orange points indicate the peak timings, whereas green points indicate the valley timings. Note that different vertical axis scales are used across the panels to improve the visibility of the time profiles.

2.3 Reply post data on SNS

We used Twitter post data as an indicator of people's anxiety (Fukuda et al., 2023). We collected news tweets posted by Yahoo! News (username: @YahooNewsTopics) and replies to these news tweets. We then performed topic analysis on the news posts to determine whether each reply was positive or negative. We focused on "Topic 3" (example words include "Tokyo," "new," "infected," "confirmed," "novel coronavirus," and "severely ill") because this topic was related to COVID-19 in Tokyo. We regarded the number of negative reply posts associated with Topic 3 news posts as a proxy of people's anxiety. The data collection period was from February 1, 2020, to May 31, 2022.

2.4 Relationship between information and anxiety

We examined the relationship between the COVID-19 data (anxiety-inducing information) and the post-data (people's anxiety). We used a 28-day centered moving average because of the large fluctuations in the post-data. As shown in Figure 1, the profiles of the COVID-19 data and the post-data repeatedly increased and decreased. Furthermore, synchronization was observed in the timing of these increases and decreases. However, while the maximum peak values in the COVID-19 data tended to increase, those in the post data tended to decrease. This indicates that anxiety-inducing information does not necessarily lead to an explosive increase in people's anxiety.

Notably, the number of negative reply posts during the third epidemic period showed a decreasing trend despite a slight increase in the number of newly confirmed COVID-19 cases. This observation suggests that anxiety may not respond to small stimuli because of habituation. Moreover, as described later, the anxiety during the third period is defined as "convergence."

Spearman's rank correlation coefficient between the COVID-19 data and the post data was calculated as $\rho = 0.196$ (p-value is $p = 0.0487$), and Kendall rank correlation was calculated as $\tau = 0.156$ (p-value is $p = 0.0202$). Therefore, the correlation between the increases and decreases in the COVID-19 data and those in the post data was statistically significant. However, this analysis was limited to identifying correlations; therefore, no causal relationship was established. In this study, we discuss the causal relationship between these two datasets using a differential equation model.

3. Model and Methodology

3.1 Model

We regarded the relationship between anxiety and habituation as analogous to an allergic-response system and proposed a set of differential equations to describe it:

$$\tau \frac{dU(t)}{dt} = \frac{P(t)(1-c)}{1+mV} - d_U U(t), \tag{1}$$

$$\frac{dV(t)}{dt} = cP(t) - d_V V(t). \tag{2}$$

In this model, $U(t)$ denotes anxiety, $V(t)$ denotes habituation to anxiety, and $P(t)$ denotes information that induces anxiety or habituation. The interactions among these variables are illustrated in Figure 2. We assumed that $P(t)$ is converted into either $U(t)$ or $V(t)$. The rate of conversion from $P(t)$ to $U(t)$ is determined by the parameter $1 - c$, where $0 < c < 1$. Accordingly, the conversion rate from $P(t)$ to $V(t)$ is given by c. Thus, the magnitude of c indicates whether $P(t)$ is more strongly transformed into anxiety or habituation. The parameter m represents the rate at which habituation suppresses the increase in anxiety. The parameters d_u and d_v correspond to the natural decay rates of anxiety and habituation, respectively. As shown in Figure 1, the peaks of negative reply posts were observed earlier than those of the COVID-19 data. Therefore, we introduce the parameter τ, which represents a time constant to improve the ability of the model to capture this phenomenon compared with our previous model (Ohno & Shoji, 2023).

In this study, we aimed to represent the relationship between information and anxiety with the model described by Eqs. (1) and (2). Specifically, our goal was to reproduce the temporal profile of negative reply posts using the anxiety variable $U(t)$, induced by the information input $P(t)$ defined from the COVID-19 data.

3.2 Simulation settings and parameter estimation

The numerical simulation results obtained from the model described by Eqs. (1) and (2) must be evaluated to determine

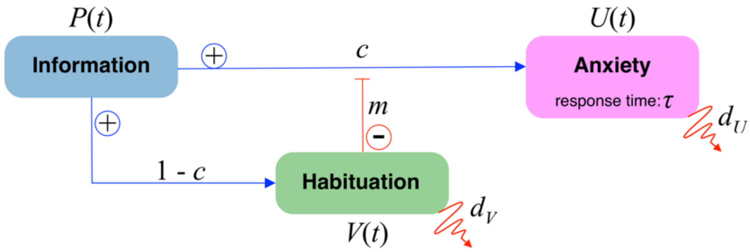

Figure 2 Schematic figure of the mathematical model for anxiety and habituation.

whether the observed phenomena are reproduced appropriately. Therefore, we formulated the problem of estimating model parameters that best reproduce these phenomena. We further analyzed the phenomena based on the estimated parameters.

Hereafter, the negative reply post data are referred to simply as the post data and are denoted by $\boldsymbol{r} = (r_1, r_2, \dots, r_n)$. To reproduce the post data, the model parameters were estimated. The parameter vector was defined as $\boldsymbol{\theta} = (c, m, \tau, d_U, d_V, U(0), V(0))$. Our objective was to estimate these parameters such that $U(t)$ reproduced the post data as accurately as possible. To achieve this, we sought the parameter value that minimized the difference between $U(t)$ and $\boldsymbol{r}$.

Bayes' theorem was applied for parameter estimation. If the probability distribution of $\boldsymbol{\theta}$ given $\boldsymbol{r}$ is obtained, the parameter set $\boldsymbol{\theta}$ that maximizes this conditional probability distribution $p(\boldsymbol{\theta}|\boldsymbol{r})$ is considered optimal. According to Bayes' theorem, the posterior probability $p(\boldsymbol{\theta}|\boldsymbol{r})$ is given by $p(\boldsymbol{\theta}|\boldsymbol{r}) \propto L(\boldsymbol{r}|\boldsymbol{\theta})p(\boldsymbol{\theta})$. Therefore, the problem reduces to maximizing the likelihood function $L(\boldsymbol{r}|\boldsymbol{\theta})$.

Let $\Phi(\boldsymbol{\theta}) = (U_1, U_2, \dots, U_n)$ denote the numerical solution obtained using an arbitrary parameter set $\boldsymbol{\theta}$. The parameter estimation problem was then treated as a regression problem between $\Phi(\boldsymbol{\theta})$ and $\boldsymbol{r}$. We defined the relative error between $\Phi(\boldsymbol{\theta})$ and $\boldsymbol{r}$ as $\eta_j = \frac{r_j - U_j}{U_j}, (j = 1,2, \dots, n)$ and assumed that $\eta_j \sim N(0, \sigma^2)$. Therefore, the likelihood function for the random variable $\boldsymbol{\eta} = (\eta_1, \eta_2, \dots, \eta_n)$ is defined as follows:

$$L(\boldsymbol{r}|\boldsymbol{\theta}) = \prod_{j=1}^{N} \left(\frac{1}{\sqrt{2\pi\sigma^2}} \exp\left\{ -\frac{\eta_j^2}{2\sigma^2} \right\} \right).$$

In this study, we set $\sigma^2 = 100.0$.

3.3 Algorithm of parameter estimation

To maximize the likelihood function $L(\boldsymbol{r}|\boldsymbol{\theta})$, we applied a Markov chain Monte Carlo (MCMC) sampling procedure (Nagayama & Matsunaga, n.d.). Through this simulation, we obtained an empirical approximation of the posterior distribution $p(\boldsymbol{\theta}|\boldsymbol{r})$.

The algorithm for parameter estimation based on MCMC simulation is described as follows:

1. Set the initial parameter value $\boldsymbol{\theta}^{(0)}$.
2. Iterate the following steps for $i = 1,2, \dots$.
3. Generate a candidate parameter set $\boldsymbol{\theta}^*$ according to the proposal distribution $q(\boldsymbol{\theta}^*|\boldsymbol{\theta}^{(i)})$.
   The proposal distribution was chosen such that random values could be generated easily, for example, a uniform distribution centered at $\boldsymbol{\theta}^{(i)}$.
4. Solve the model defined by Eqs. (1) and (2) numerically using $\boldsymbol{\theta}^*$, and compute the likelihood $L(\boldsymbol{r}|\boldsymbol{\theta}^*)$.
5. Update the parameter according to the following rule:

$$\theta^{(i+1)} = \begin{cases} \theta^* & if\ \mathrm{x} \le a(\boldsymbol{\theta}^*|\boldsymbol{\theta}^{(i)}), \\ \theta^{(i)} & if\ \mathrm{x} > a(\boldsymbol{\theta}^*|\boldsymbol{\theta}^{(i)}), \end{cases}$$

   where

$$a(\boldsymbol{\theta}^*|\boldsymbol{\theta}^{(i)}) = \min\left\{1, \frac{L(\boldsymbol{r}|\boldsymbol{\theta}^*)}{L(\boldsymbol{r}|\boldsymbol{\theta}^{(i)})}\right\}.$$

   Here, x is a random number drawn from a uniform distribution over the interval $[0,1]$.

The MCMC simulation was performed for a sufficiently large number of iterations. However, during the initial phase of the simulation, the sampled values of $\boldsymbol{\theta}$ were unstable. Therefore, samples obtained in this initial phase were discarded and excluded from the final parameter value estimation. In this study, the MCMC simulation was run for 500,000 iterations, with the first 200,000 iterations discarded as burn-in.

We performed interval estimation of the parameters using the MCMC simulation results. As the parameters must be evaluated as a combination, the sampled parameter sets were assessed collectively. Parameter sets sampled several times were considered more likely to be adopted. However, frequently sampled locally optimal parameter sets should not necessarily be adopted. Conversely, parameter sets located in high-density regions of the posterior distribution should be considered, even if sampled less frequently. Therefore, we calculated the density of each parameter set in the parameter space using the k −nearest neighbor (k −NN) method. The parameter sets were sorted according to the density scores calculated by the k −NN method, and the cumulative density was defined as the cumulative sum of the relative sampling frequencies in descending order of the density scores. Parameter sets included within 95% of the cumulative density were regarded as belonging to the confidence interval. In this study, we set $k = 100$ as the k −NN method.

4. Result and Analysis

4.1 Numerical simulation result

The models defined by Eqs. (1) and (2) were numerically simulated using the fourth-order Runge-Kutta method with a time step of $dt = 0.01$. The parameter set $\boldsymbol{\theta}$ was estimated using MCMC simulation. Parameters were estimated using the reply post data from the k −th epidemic period, and simulations were performed for epidemic periods after the $(k+1)-$th period. As the initial parameter values $\theta^{(0)}$ for the MCMC simulation, we set $(c, m, \tau, d_U, d_V) = (0.9, 0.9, 1.0, 0.05, 0.05)$. The initial value $U(0)$ was set to the first observed value in the $k-$th period. For the $(k+1)$ −th period, $V(0)$ was set to the simulated value of $V(t)$ at the beginning of the $(k+1)$ −th period obtained from the simulation for the k −th period. For the first period, $V(0)$ was set to 0.0.

The numerical simulation results are shown in Figure 3. As a general trend, the peak value of the anxiety variable $U(t)$ decreased even when the information input $P(t)$ increased. When the first epidemic period was used as the training data, $U(t)$ increases significantly during the first epidemic period. However, during the second, third, fourth, and fifth epidemic periods, the increases in $U(t)$ were relatively small. Moreover, the value of $U(t)$ during the fifth epidemic period was higher than that during the fourth epidemic period. This tendency was consistent with the post data. Similar trends were also observed when other epidemic periods were used as the training data.

4.2 Estimated parameters

Figure 4 presents boxplots of the estimated parameters for each epidemic period. The parameter values varied depending on the learning period. For on parameter c, its values during the first, second, and third epidemic periods were smaller than those during the fourth and fifth periods. As c represents the conversion rate of information into anxiety or habituation, this result indicates that people gradually developed greater habituation to information over time.

The time constant τ was frequently sampled with values smaller than 1 during the first, second, fourth, and fifth epidemic periods. This finding suggests that the response of anxiety was faster than that of habituation. In contrast, the model was trained on the third epidemic period, τ was frequently sampled with values greater than 1 because the observed anxiety exhibited only gradual changes during this period.

The decay rates d_U and d_V were consistently sampled with small values across all learning periods. However, d_U was frequently sampled with higher values when using the third period for learning data than when using the other epidemic periods. This result was likely influenced by a decreasing trend in the post data during the third period. The initial values $U(0)$ and $V(0)$ were sampled close to their initial settings.

4.3 Analysis

We analyzed the numerical simulation results to evaluate the reproducibility and utility of the model.

4.3.1 Comparison of peak timing

We evaluated whether the model could reproduce the peak dates in the post data. Each peak date was defined as the date on which the maximum value is observed during each epidemic period. Table 2 presents the comparison of peak dates between the post data and the model results. A difference of one week was considered an acceptable error because the post data were aggregated weekly.

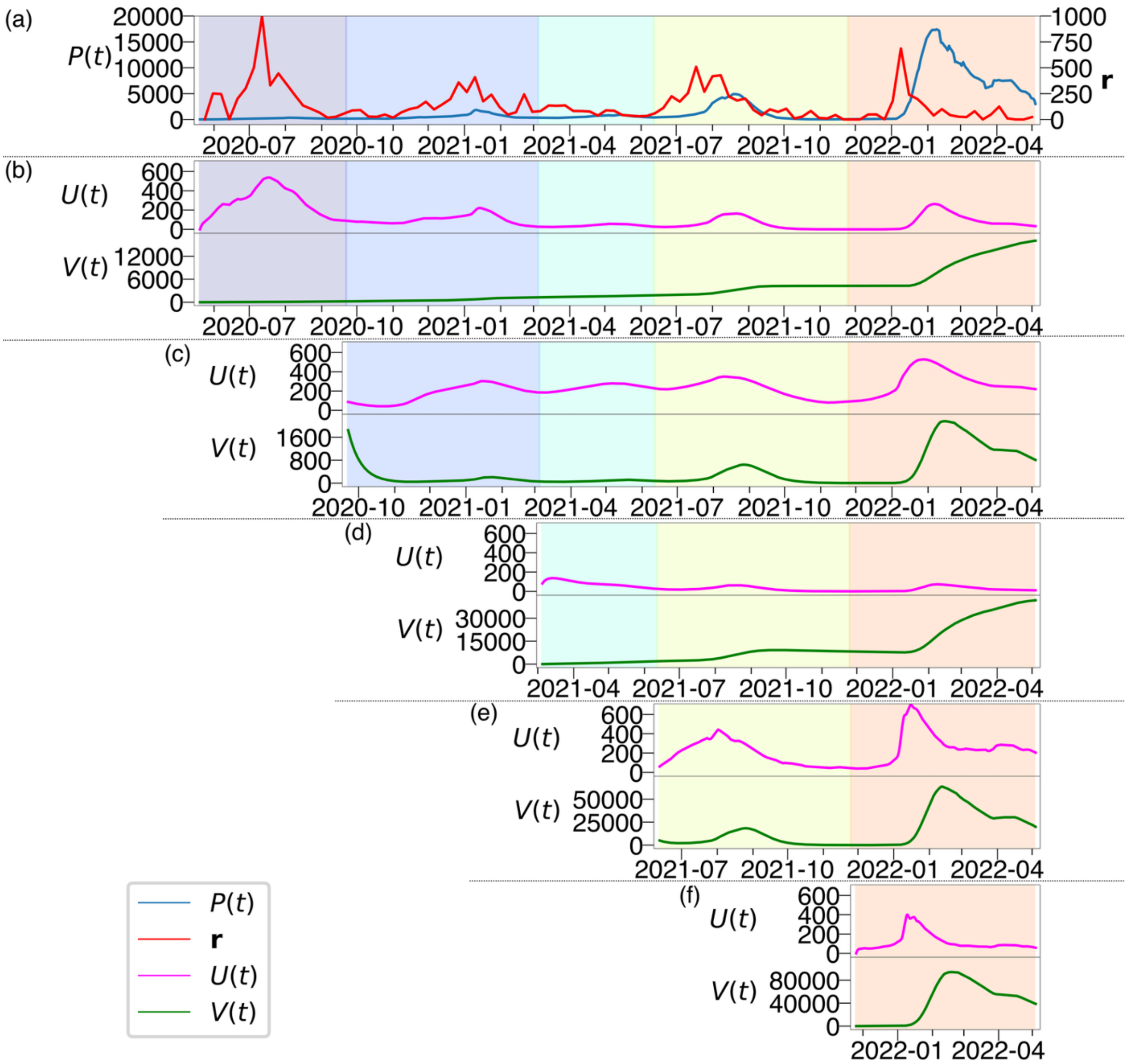

Figure 3 Real dynamics of anxiety for the mathematical model defined by Eqs. (1) and (2). Panel (a) shows the newly confirmed COVID-19 cases as the input information, $P(t)$ (blue line), and the number of negative reply posts as the post data, r_t (red line). Panels (b)–(f) show the simulation results obtained using the first through fifth learning periods, respectively. In panels (b)–(f), the magenta and green lines represent anxiety ($U(t)$) and habituation ($V(t)$), respectively. Note that the vertical axis scale for $V(t)$ differs among panels (b)–(f) to improve visibility.

The model exhibited a tendency to forecast the peak dates of the epidemic periods following the learning period. This result suggests that the model can provide short-term forecasts. Differences of approximately one month were observed in the forecasts for the fourth and fifth periods when the first or second epidemic period was used as the learning period. Over time, people's anxiety responses to information may gradually change.

4.3.2 Convergence of anxiety

We examined whether the model could reproduce gradual changes in the time series. Here, we define "convergence" for anxiety values and compare the periods of convergence between the post data and the model results.

As a measure of gradual change, the local variance $(\sigma^2)_k^{\mathrm{local}}$ is defined as follows:

$$(\sigma^2)_k^{\mathrm{local}} = \frac{1}{2m+1}\sum_{i=k-m}^{k+m}\left(X_i - \overline{X}_k\right)^2,\ \overline{X}_k = \frac{1}{2m+1}\sum_{i=k-m}^{k+m} X_k.$$

We define the state as "convergence" when the anxiety value X_k (i.e., r_k or U_k) is lower than a threshold $\varepsilon_{\mathrm{level}}$, and the

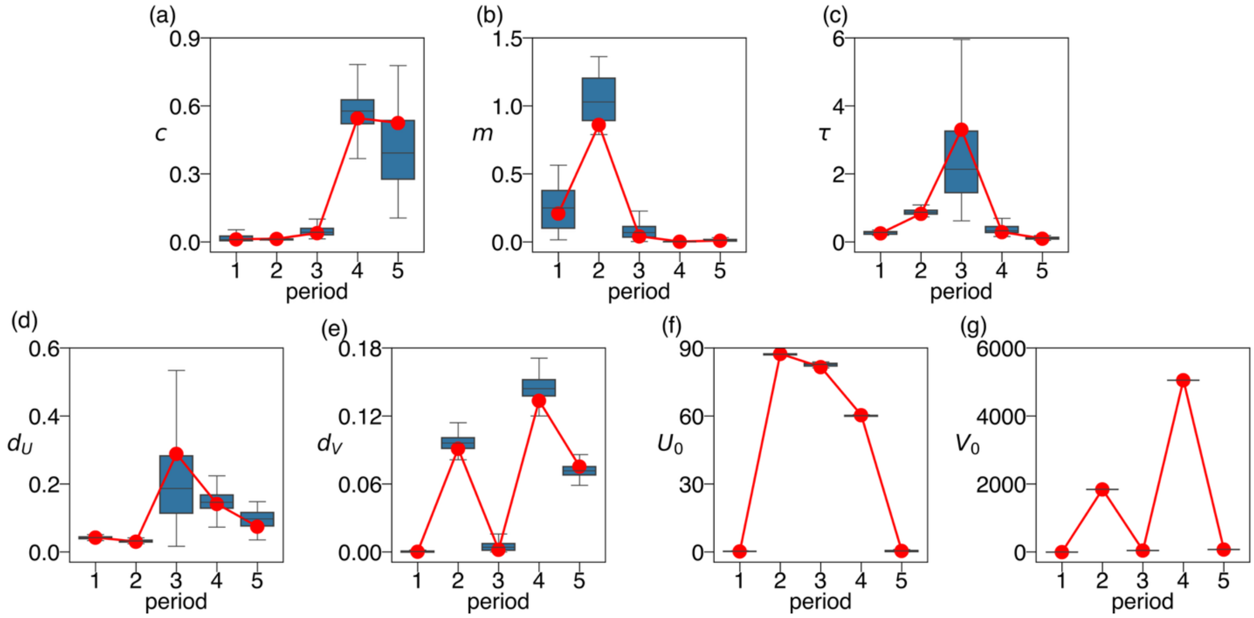

Figure 4 Boxplots of estimated parameters. Boxplots are shown without plotting individual outliers for clarity. Panels (a)–(g) correspond to the estimated parameters $c, m, d_U, d_V, \tau, U(0)$, and $V(0)$, respectively. The horizontal axis indicates the learning period, and the vertical axis indicates the parameter value. The red line indicates the parameter value with the highest estimated density among the posterior samples.

Table 2 The peak date of each epidemic period. Rows represent epidemic period. The left most column shows the post data, whereas the remaining columns show the results of the model when the first, second, third, and fourth epidemic periods were used as the learning periods. Lag indicates the difference in days between the post data and the model results.

	post data	1st	Lag	2nd	Lag	3rd	Lag	4th	Lag	5th	Lag
1st	2020/7/12	2020/7/18	6								
2nd	2021/1/10	2021/1/13	3	2021/1/15	5						
3rd	2021/3/28	2021/5/15	48	2021/5/4	37	2021/3/13	-15				
4th	2021/7/18	2021/8/20	33	2021/8/10	23	2021/8/10	32	2021/8/1	14		
5th	2022/1/9	2022/2/6	28	2022/1/27	18	2022/2/9	31	2022/1/16	7	2022/1/9	0

local variance $(\sigma^2)_k^{\text{local}}$ is lower than a threshold ε_σ:

$$X_k < \varepsilon_{\text{level}} \; and \; (\sigma^2)_k^{\text{local}} < \varepsilon_{\sigma.}$$

The convergence results based on this evaluation measure are shown in Figure 5, and the comparison of the convergence periods between the post data and the model results is presented in Table 3. Here, $\varepsilon_{\text{level}}$ and ε_σ are set to 20% of the maximum value of X. For the post data,

$$\varepsilon_{\text{level}} = 0.2 \max_k r_k \, , \; \varepsilon_\sigma = 0.2 \max_k (\sigma^2)_k^{\text{local}}.$$

For the simulation data, the threshold parameters were adjusted according to each epidemic period:

$$\varepsilon_{\text{level},k} = 0.2 \max_{i \in k\text{−th period}} U_i \, , \; \varepsilon_{\sigma,k} = 0.2 \max_{i \in k\text{−th period}} (\sigma^2)_i^{\text{local}}.$$

In the post data, the third period was classified as “convergence.” During this period, habituation appeared to surpass anxiety, even though the number of newly confirmed COVID-19 cases slightly increased. Furthermore, the anxiety dynamics in the third period exhibited a transition distinct from those of the other periods.

When the first epidemic period was used as the learning period, convergence was observed at approximately the same time as in the post data, although the model tended to overestimate the duration of convergence. When the second period was used as the learning period, convergence was not reproduced because anxiety did not decrease sufficiently during the third period. However, as previously mentioned, the third period has a distinctive profile, making reproduction and forecasting difficult. For a similar reason, when the third period was used as the learning period, it was not classified as a convergence in the simulation results. In contrast, the forecasts for the fourth and fifth periods were classified as convergent. When the fourth period was used as the learning period, convergence between the fourth and fifth period

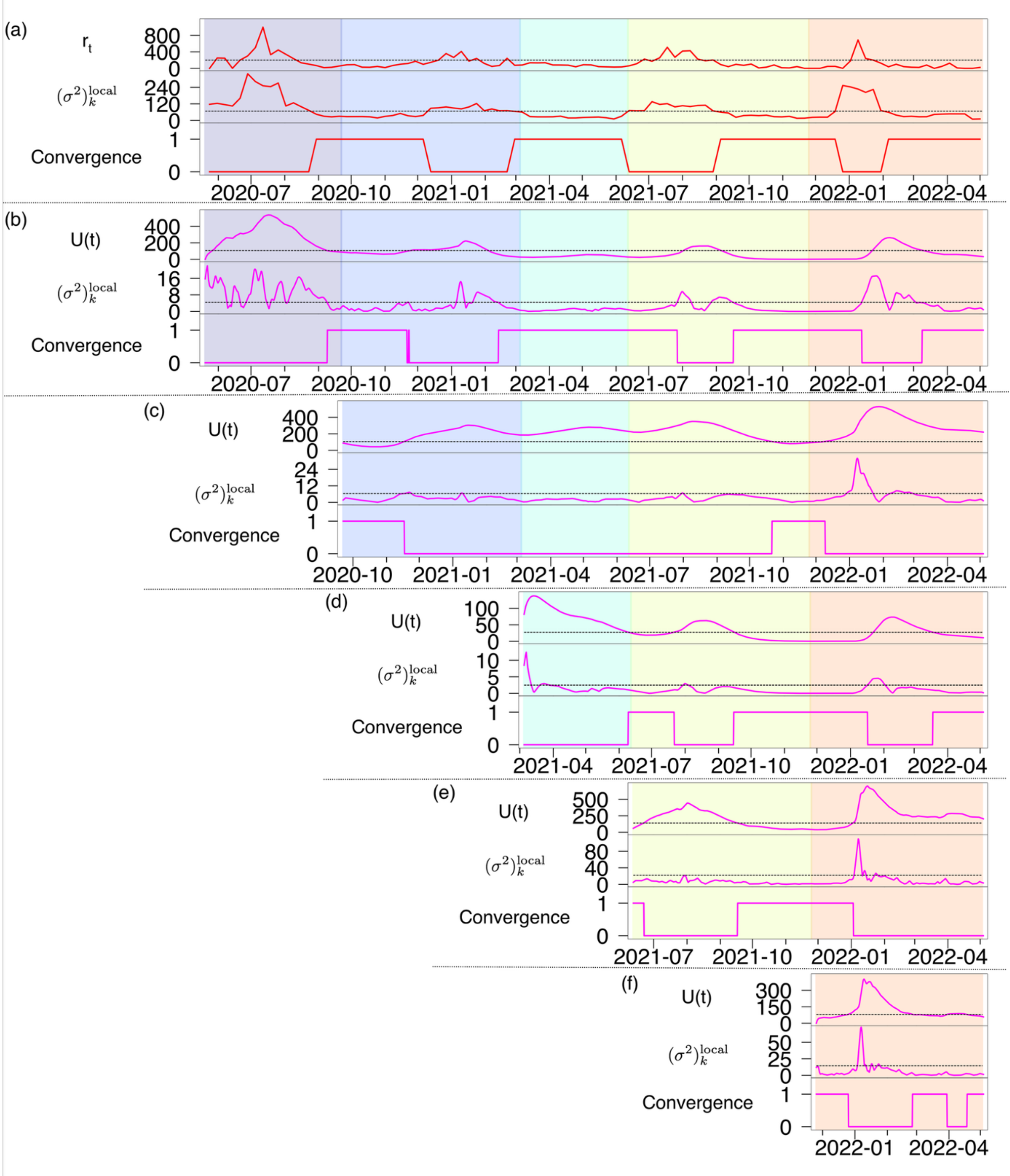

Figure 5 Time profiles of results for analysis of "convergence." Panel (a) shows the observed anxiety (top), its local variance (middle), and the corresponding convergence judgment (bottom). Panels (b)–(f) show the simulated anxiety (top), its local variance (middle), and the corresponding convergence judgment (bottom), obtained using the first through fifth learning periods, respectively. The dashed lines in the top and middle plots represent the threshold values $\varepsilon_{\mathrm{level}}$ and ε_{σ}, respectively, used for the convergence criterion.

could be reproduced.

From this analysis, although convergence was overestimated or not reproduced in some cases, the model was nevertheless capable of reproducing convergence behavior. In particular, the simulation results obtained using the first period as learning data were consistent with the post data.

4.3.3 Definition of the rate of decrease

We defined the rate of decrease, ρ, to evaluate the decreasing trend of anxiety in response to information:

Table 3 Start and end dates of the convergence periods identified for the post data and the simulation results obtained using each learning period.

post data		1st		2nd		3rd		4th		5th	
Start date	**End date**	**Start date**	**End date**	**Start date**	**End date**	**Start date**	**End date**	**Start date**	**End date**	**Start date**	**End date**
2020/8/30	2020/12/6	2020/9/8	2020/11/23	2020/9/22	2020/11/17						
2021/2/28	2021/6/6	2021/2/12	2021/7/27			2021/6/9	2021/7/21	2021/6/12	2021/6/21		
2021/9/16	2021/12/12	2021/9/16	2022/1/12	2021/10/21	2021/12/9	2021/9/14	2021/1/22	2021/9/16	2021/1/2	2021/11/25	2021/12/25
2022/2/6	2022/4/24	2022/3/8	2022/5/3			2022/3/18	2022/5/3	2022/2/24	2022/3/29		

$$\rho_{kl}(X) = \frac{X_l^{\text{high}} - X_k^{\text{high}}}{X_k^{\text{high}}},\ X_k^{\text{high}} = \max_{i \in k\text{−th period}} X_i.$$

Here, X denotes either r or U. Figure 6 illustrates the heat map of the decreasing rates for the post data and simulation results obtained using different learning periods. The rows represent the reference periods corresponding to k, whereas the columns represent the comparison periods corresponding to l. A negative value of ρ indicates a decreasing trend, and the corresponding cells are colored blue. In contrast, a positive value of ρ indicates an increasing trend, and the corresponding cells are colored red.

In the post data, $\rho_{1l}(r)$ showed a decreasing trend. In contrast, increasing trends were observed for the fourth and fifth epidemic periods ($\rho_{k4}(r)$ or $\rho_{k5}(r)$) when the reference period was any period other than the first period.

In the simulation results, $\rho_{lk}(U)$ was generally consistent with the post data. When the first period was used as the learning period, $\rho_{lk}(U)$ was similar to $\rho_{lk}(r)$. Therefore, the model could forecast both decreasing and increasing trends. When the second period was used as the learning period, the increasing trends for $k = 2$ differed between the model and the post data. However, the increasing trends for $k = 3$ and $k = 4$ (i.e., when the reference periods were the third and fourth periods) were consistent with the post data. When the third period was used as the learning period, differences between the model and post data were observed because of the distinctive characteristics of the third period. When the fourth period was used as the learning period, the peak value in the fifth period could be forecast as an increasing trend.

Overall, the numerical simulations exhibited trends similar to those of the post data. Therefore, our model successfully represented the decreasing trend in anxiety despite the increasing trend in COVID-19 cases.

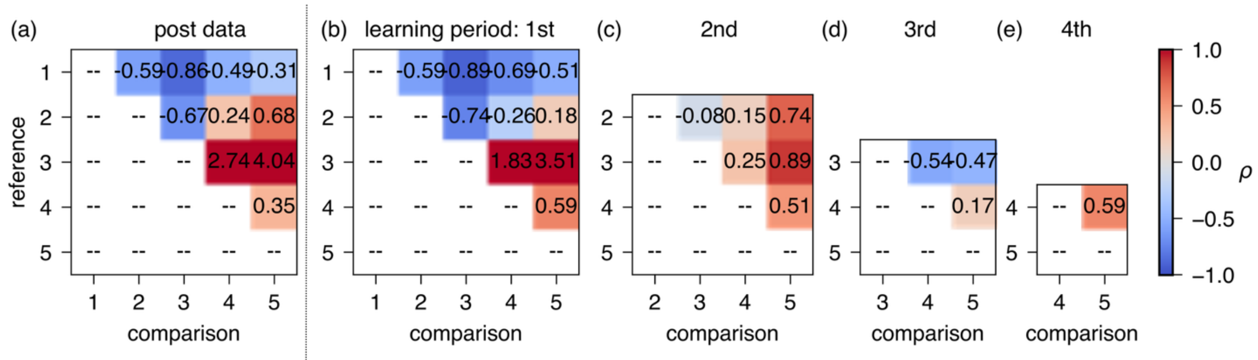

Figure 6 Heat maps showing the results of decrease-rate analysis. Panel (a) shows the analysis result for the post data. Panels (b)–(e) show the analysis results obtained using the first through fourth learning periods, respectively. In each heat map, the vertical axis indicates the reference period, and the horizontal axis indicates the comparison period. Each cell is colored according to the rate of decrease, ρ, with positive values shown in blue and negative values shown in red. The numerical value in each cell indicates the corresponding value of ρ.

5. Discussion

We discuss trends in the reproducibility of anxiety in the simulation results. As shown in Figure 3, the anxiety variable in the model increased and decreased in response to COVID-19 information. Furthermore, the peak values gradually decreased over time. This result indicates that repeated exposure to anxiety-inducing information gradually enhances habituation.

To evaluate the reproducibility of the decreasing trend in peak values, we compared peak timing, defined anxiety convergence and defined the rate of decrease. The results from the comparison of the peak timings between the model and the post data indicates that the model can provide short-term forecasts (Table 2). This suggests that long-term forecasting is difficult because the dynamics of anxiety evolve over time.

From the estimated model parameters (Figure 4), the conversion rate from information to anxiety and the suppression effect of habituation exhibited different trends between the first–third periods and the fourth–fifth periods. These results suggest that peak timings in the fourth and fifth periods cannot be accurately predicted when the second period is used as the learning period. Therefore, long-term forecasting remains a challenge in this study.

By defining the “convergence” of anxiety, we can discuss not only increases in anxiety but also periods during which anxiety converges. According to our definition, the third period is classified as a convergence period in the post data. During this period, the number of confirmed COVID-19 cases increased less than in the other periods, whereas anxiety in the post data showed a decreasing trend. This discrepancy suggests that anxiety did not increase in response to small stimuli because habituation had already accumulated sufficiently during the first and second periods.

In the simulation results, the third period was classified as “convergence” when the first period was used as the learning period. However, when the third period was used as the learning period, the simulation results indicate only a small increase in anxiety. This is because the model parameters were estimated based on the characteristics of the convergence period.

In the simulation results, to the model tended to produce increases in anxiety even in response to small stimuli. This is an inherent characteristic of our model because the number of newly confirmed COVID-19 cases was used as the input information. Therefore, reproducing the decreasing trend observed in the third period of the post data remains challenging. This limitation should be addressed in future improvements of the model.

To examine the decrease in peak values, we compared increasing and decreasing trends of the peak values between the model and post data (Figure 6). Our results revealed that the model generally reproduced the trends in the post data. This suggests that the model can represent the gradual decreases in anxiety responses over time. We can infer that suppression through habituation is implicitly embedded in the dynamics of anxiety.

6. Conclusion

We proposed a mathematical simulation model for anxiety based on an allergic-response framework. In our previous work, the application of the mathematical model to real-world phenomena was identified as a remaining issue (Ohno & Shoji, 2023). In this study, we refined the model using post data, and the revised model qualitatively reproduced the dynamics of real-world anxiety (Figure 3). These results suggest that habituation is implicitly embedded in anxiety dynamics and support the hypothesis that the interaction between anxiety and habituation resembles an allergic mechanism.

We extracted numerical data representing anxiety and the information that induces it. However, a mathematical model is necessary for the underlying habituation process. In this study, habituation is explicitly incorporate into the model; therefore, the model can be regarded as describing the emotional dynamics of anxiety.

The model parameters were appropriately estimated using data assimilation. The results show that parameter values change across epidemic periods. Over time, information appears to contribute more to the increase in habituation than to anxiety. This result is consistent with the observation that people’s anxiety became less sensitive to increases in COVID-19 cases during the pandemic.

In this study, the model was based on the analogy that the relationship between anxiety and habituation resembles an allergic system. Various studies have investigated the dynamics of anxiety and emotions using frameworks such as the free-energy principle and information diffusion models based on epidemic processes (Ueda et al., 2021, and Bartkow et al., 2023). However, mathematical modeling of the dynamics and interactions of multiple emotions (i.e., KANSEI dynamics) remains under development. Our results suggest that the dynamics of anxiety and habituation can be interpreted through an allergic-system analogy. Nevertheless, several issues remain for future work, including incorporating conservation laws, such as energy conservation, into agent-based simulations based on this framework.

We also found that changes in the learning data lead to changes in the optimal parameter set. This result suggests that model parameters vary over time. Therefore, the dynamics of anxiety may be more accurately reproduced by combining data assimilation with a model that incorporates time-varying parameters. Understanding temporal changes in parameters may help clarify how people process information and experience anxiety over time.

This study has significance for one of the proposals of a mathematical model for KANSEI dynamics (Ohno & Shoji, 2023). Further discussion of KANSEI dynamics will remain an important direction for future research.

Ethics Statement

Not applicable.

Author Contributions

K.O. and H.S. conceived and designed the study. K.O. and K.S. formulated the mathematical model and performed data analysis. S.F. collected the SNS data. K.O. developed the simulation framework, performed the numerical simulations, and wrote the manuscript. H.S., K.S. and S.F. reviewed the manuscript. All authors contributed to the manuscript revision and have read and approved the submitted version.

Funding

This work was supported by Chuo University Joint Research Grant.

Conflict of Interest

The authors declare that they have no conflict of interest.

Acknowledgements

The authors thank Dr. M. Ohkura for the valuable discussions related to this study.

Notes

In this study, ChatGPT was used to refine the English manuscript and improve the computational code. All outputs were reviewed and verified by the authors.

References

Horn G. (1967). Neuronal Mechanisms of Habituation, *Nature, 215*, 707–711. https://doi.org/10.1038/215707a0

Ariga A. and Lleras A. (2011). Brief and rare mental "breaks" keep you focused: Deactivation and reactivation of task goals preempt vigilance decrements. *Cognition*, *118(3)*, 439-443. https://doi.org/10.1016/j.cognition.2010.12.007

Stanley J. (1976). Computer simulation of a model of habituation. *Nature, 261*, 146–148. https://doi.org/10.1038/261146a0

Ueda K, Sekoguchi T, and Yanagisawa H (2021). How predictability affects habituation to novelty. *PLoS ONE 16(6)*, e0237278. https://doi.org/10.1371/journal.pone.0237278

Bartkow P, Bortko K, Jankowski J, and Pazura P (2023). Modeling the impact of the habituation effect on information spreading processes with repeated contacts under an SI model. *PLoS ONE 18(4)*, e0280266. https://doi.org/10.1371/journal.pone.0286690

Ohno, K. and Shoji, H. (2023). Mathematical modeling of KANSEI dynamics for anxiety based in allergy model. *2023 IEEE International Conference on Systems, Man, and Cybernetics (SMC), Honolulu, Oahu, HI, USA, 2023,* 4581-4586. https://doi.org/10.1109/smc53992.2023.10394431

Fishman M.A. and Segel L.A. (1996). Modeling Immunotherapy for Allergy. *Bulletin of Mathematical Biology*, *58(6)*, 1099-1121. https://doi.org/10.1016/S0092-8240(96)00036-5

Groß F, Metzner G, and Behn U (2011). Mathematical modeling of allergy and specific immunotherapy: Th1–Th2–Treg interactions, *J. Theo. Bio. 269*, 70–78. https://doi.org/10.1016/j.jtbi.2010.10.013

Hara A. and Iwasa Y. (2017). When is allergen immunotherapy effective? *J. Theo. Bio*. *425*, 23–42. https://doi.org/10.1016/j.jtbi.2017.04.030

Ministry of Health, Labour and Welfare. (n.d.). *Trend in the number of newly confirmed cases (daily)*. Ministry of Health, Labour and Welfare. Retrieved May 29, 2025, from https://covid19.mhlw.go.jp/public/opendata/confirmed_cases_cumulative_daily.csv

Fukuda S., Nanba H., and Shoji H. (2023). An Analysis of Shifts in Public Interests and Sentiments in Japan Using News Tweet Data during the COVID-19 Pandemic. *14th IIAI International Congress on Advanced Applied Informatics (IIAI-AAI), Koriyama, Japan, 2023*, 106-111. https://doi.org/10.1109/IIAI-AAI59060.2023.00030

Nagayama, M., & Matsunaga, S. (n.d.). *Parameter estimation for mathematical models* [PowerPoint slides]. Hokkaido University. https://mmc01.es.hokudai.ac.jp/wp/wp-content/uploads/2020/06/Intro_Para_Estimation.pdf